Journal of Chemometrics

WILEY

Journal of CHEMOMETRICS

RESEARCH ARTICLE

The FTIR-ATR Spectroscopy as a Biosensing Strategy for Thermal Effects in Permissibility Verification of Lard-Adulterated Palm Oil

Muhammad Zulhelmi Nazri[1,2] | Dayang Norulfairuz Abang Zaidel[1,2] | Muhamad Shirwan Abdullah Sani[3] | Hajar Aminah A. Karim[2] | Siti Nor Azlina Abd Rashid[2,4] | Anjar Windarsih[5]

[1]Malaysia-Japan International Institute of Technology (MJIIT), Universiti Teknologi Malaysia (UTM), Kuala Lumpur, Malaysia | [2]Innovation Centre in Agritechnology for Advanced Bioprocessing (ICA), Universiti Teknologi Malaysia (UTM), Pagoh, Johor, Malaysia | [3]International Institute for Halal Research and Training (INHART), Level 3, KICT Building, International Islamic University Malaysia (IIUM), Kuala Lumpur, Malaysia | [4]Innovation and Commercialization Centre (ICC), Office of Deputy Vice Chancellor (Research & Innovation), Universiti Teknologi Malaysia (UTM), Kuala Lumpur, Malaysia | [5]Research Centre in Food Technology & Processing (PRTPP), National Research and Innovation Agency (BRIN), Yogyakarta, Indonesia

Correspondence: Dayang Norulfairuz Abang Zaidel (dnorulfairuz@utm.my)

Received: 15 January 2026 | **Revised:** 4 May 2026 | **Accepted:** 6 May 2026

Keywords: chemometric analysis | FTIR-ATR spectroscopy | lard adulteration | permissibility authentication | spectral biosensing

ABSTRACT

Ensuring authenticity of edible oils is vital for consumer trust, regulatory compliance and permissibility assurance, particularly for Muslim consumers. This study introduces a spectral biosensing strategy using Fourier transform infrared spectroscopy coupled with attenuated total reflectance (FTIR-ATR) and chemometric modelling to detect lard adulteration in palm oil (PO) under thermal stress. PO samples spiked with 1%–50% v/v lard were heated from 25°C to 200°C for 30 min, simulating industrial and culinary conditions. FTIR-ATR spectra showed distinct shifts in carbonyl and fingerprint regions due to lard incorporation and heat-induced lipid degradation. Discriminant analysis (DA) achieved 100% classification accuracy across the full spectrum (4000–650 cm^{-1}), demonstrating strong discriminatory power. Partial least squares–discriminant analysis (PLS-DA) identified the fingerprint region (1000–650 cm^{-1}) as most diagnostic, yielding robust performance with $R^2Y = 0.895$, $R^2X = 1.000$, $Q^2 = 0.893$ and 100% correct classification in both training and validation datasets. Principal component analysis (PCA) revealed clear clustering of pure and adulterated samples, even under severe thermal conditions. Moreover, using the optimised FTIR-ATR/PLS model, the lard adulteration in thermally treated PO could be reliably detected at levels as low as 1% *v/v* with LOD and LOQ ranges of 0.01%–1.14% and 0.02%–3.34% v/v, respectively. These findings position FTIR-ATR with multivariate chemometrics as a rapid, nondestructive and thermally resilient platform for lard detection in PO. The approach extends to broader food quality and safety monitoring in real-world processing scenarios.

1 | Introduction

Food adulteration is a critical global concern that undermines consumer trust; compromises food quality, especially in the case of permissibility products; and poses serious religious and ethical implications [1, 2]. Among many edible oils, palm oil (PO) is particularly vulnerable to adulteration with lard due to its similar physico-chemical characteristics, making detection through conventional methods challenging [3]. For Muslim consumers, the presence of porcine derivatives such as lard in food products is strictly prohibited, thereby necessitating reliable and robust analytical approaches for permissibility authentication [4].

In recent years, Fourier transform infrared spectroscopy coupled with attenuated total reflectance (FTIR-ATR) has emerged as a promising biosensing technology for authentication of

edible oils and fats. Unlike conventional wet chemistry assays or conventional separation techniques such as gas and liquid chromatography, FTIR-ATR is rapid and non-destructive instrument and requires minimal sample preparation, while simultaneously offering molecular-level information through the vibrational signatures of the fatty acid properties in the samples [5, 6]. These properties align FTIR-ATR with the broader category of biosensing spectral technologies, as it enables sensitive, label-free detection of biochemical changes in complex food matrices, particularly when integrated with chemometric modelling [7, 8]. In this context, biosensing does not necessarily require a biological recognition element but encompasses spectral sensing approaches capable of identifying biomarkers or adulterants relevant to food safety and authentication [9, 10].

The application of FTIR-ATR to edible oils has been widely reported, with successful discrimination of adulterated from pure samples achieved through chemometrics such as principal component analysis (PCA), discriminant analysis (DA) and partial least squares–discriminant analysis (PLS-DA) [11, 12]. Particularly, the fingerprint region (1000–650 cm^{-1}) of the FTIR spectrum is highly diagnostic, capturing compound-specific vibrations that differentiate animal fats from vegetable oils [13, 14]. However, the impact of thermal processing, which is a common step in food preparation, on the spectral integrity and classification performance of such biosensing strategies remains underexplored. Because thermal treatment can induce lipid oxidation, degradation and structural rearrangements, understanding its influence is essential for developing thermally resilient permissibility verification methods [15, 16].

Accordingly, this study investigates the potential of FTIR-ATR spectroscopy as a spectral biosensing technology to detect lard adulteration in palm oil exposed to various thermal treatments. The approach utilises the sensitivity of vibrational spectroscopy as part of the biosensing technology that is able to capture subtle molecular fingerprints associated with lipid structural variations while integrating advanced multivariate chemometric analysis to enhance discrimination and classification accuracy. Establishing by robust, rapid and non-destructive analytical instrument, this work not only addresses critical and crucial requirement for permissibility verification or authentication but also contributes significantly to the broader domain of biosensing technologies, particularly in ensuring food authenticity, quality assurance and safety monitoring in complex processing environments.

2 | Materials and Methods

2.1 | Materials

Palm oil (brand: Vesawit, origin: Malaysia) was purchased from a local grocery store in Pagoh, Johor, Malaysia. Standard lard and palm oil were purchased from Sigma-Aldrich, United States, whereas ethanol was purchased from R&M Chemicals, United Kingdom. The standard lard and palm oil were of analytical grade and were used as supplied without further processing.

2.2 | Heat Treatment of Oil Samples

To prepare the adulterated samples, lard was mixed into PO at various concentrations of 1%, 5%, 10%, 20%, 30%, 40% and 50% (*v*/*v*), whereas standard PO and lard oil were used as the oil controls. Each mixture was homogenised with constant stirring to ensure uniform distribution of the lard in the palm oil matrix. Oil samples at 25°C were used as the control temperature. The samples were then heat treated for 30 min at different cooking temperatures of 50°C, 100°C, 150°C and 200°C to stimulate standard thermal processing conditions.

2.3 | Colour Analysis

All oil-adulterated samples were subjected to colour analysis with a colorimeter (Hisuc, China). The evaluation focused on the assessment of changes in visual properties, especially colour and clarity. This evaluation was based on the CIE colour space system, in which L^* indicates the degree of lightness, a^* represents the red-green spectrum and b^* corresponds to the yellow-blue spectrum. These parameters provide a quantitative measure of the colour variations that are influenced by thermal processing.

2.4 | The FTIR-ATR Measurement

The FTIR measurement of the individual oil-adulterated samples after heating treatments was recorded in the wavenumber of 4000–650 cm^{-1} range at ambient temperature of 25°C, respectively. For each spectrum, 32 scans were accumulated using the FTIR-ATR Nicolet iS5 instrument (Thermo Scientific, United States). The spectral data were processed using OMNIC software (Thermo Scientific, United States) with a moving mirror optical velocity of 0.4747 $cm\,s^{-1}$ and Happ-Genzel apodisation. The phase correction was performed using the Mertz method. The IR measurement was performed with a resolution of 4 cm^{-1}. The ATR diamond was carefully cleaned with ethanol between every individual measurement and dried before new samples were applied.

2.5 | Multivariate Analysis of Variance

2.5.1 | Dataset Preprocessing

The FTIR-ATR spectra were acquired in a CSV (Comma-Separated Values) file using Microsoft Excel and then exported to XLSTAT software (Version 2019, France) [17]. The preprocessing steps included outlier detection, data transformation and a test for adequacy of the data set with a significance level of $\alpha = 0.01$. The spectral transmittances were divided into seven different wavenumber ranges: 1000–650, 1500–1001, 2000–1501, 2500–2001, 3000–2501, 3500–3001 and 4000–3501 cm^{-1}. These regions were identified through a systematic two-step approach. First, the FTIR-ATR spectra were visually inspected using OMNIC software (Thermo Scientific, United States) and absorption bands were assigned to functional groups based on established lipid FTIR literature including the C–H stretching (3000–2800 cm^{-1}), carbonyl C=O stretching (1744 cm^{-1}) and fingerprint regions of 1000–650 cm^{-1}. Second, the full spectrum was systematically segmented into seven equal-width

regions to ensure unbiased coverage of all chemically relevant windows. Chemometric models (DA, PLS-DA and PCA) were then independently applied to each region, and the most diagnostic spectral window was identified based on model performance metrics (R^2Y, Q^2 and classification accuracy). This approach ensured that region selection was both chemically justified and empirically validated.

2.5.2 | The Kaiser–Meyer–Olkin (KMO) Test

All preprocessed data were subjected to the KMO test at a significant level of $\alpha = 0.01$ to assess their suitability for latent variable extraction. The resulting KMO statistic was interpreted against established benchmarks: KMO < 0.5 denoted an inadequate dataset; those $0.5 <$ KMO < 0.7 were deemed passable; $0.7 <$ KMO < 0.8 were classified as good; $0.8 <$ KMO < 0.9 indicated a very good dataset; and KMO > 0.9 were considered excellent. The stringent evaluation ensured that only datasets meeting the predefined adequacy criteria advanced to subsequent multivariate analyses.

2.5.3 | Dataset Transformation

Prior to conducting PCA, the distributional properties of the preprocessed dataset were rigorously evaluated to ensure compliance with the assumption of normality. Specifically, the Shapiro–Wilk test was applied at a stringent significant threshold of $\alpha = 0.01$, whereby any series of measurement yielding a p value below this cutoff would indicate a departure from normality. To mitigate such deviations and achieve a standardised scale across variables, the dataset was then subjected to a transformation using the unbiased $(n-1)$ standard deviation method. This two-step procedure of normality testing followed by variance-standardising transformation both safeguarded the integrity of the PCA and optimised the extraction of meaningful principal components (PCs) for downstream multivariate interpretation.

2.5.4 | The Discriminant Analysis

The DA was used to develop a model that distinguishes between pure and adulterated PO with lard samples at different temperature using the FTIR spectra. A 'cluster' label was added to the datasets to classify samples as either blank or adulterated. The model, built at a significance level of $\alpha = 0.01$, combined spectral features with the 4000–650 cm^{-1} range to separate the sample groups. Statistical tests, including F statistics and Wilks' lambda p values were used to identify significant spectral differences. The model's classification accuracy was validated using training and cross-validation datasets, and the differences between blank and adulterated samples were confirmed through Fisher distance values and associated p values.

2.5.5 | The Partial Least Squares–Discriminant Analysis

The PLS-DA was used to develop a model for identifying adulteration in PO and lard samples at different temperature using the FTIR spectra. A 'cluster' label was added to the datasets to classify samples as either blank or adulterated. The PLS-DA was performed at a significance level of $\alpha = 0.01$, projecting the spectral data onto a latent variable space optimised to distinguish between classes. The model assigned each sample to a class based on its FTIR spectrum and calculated discriminant scores for classification. The model's performance was evaluated using several metrics: R^2Y (goodness-of-fit to the response), R^2X (variance explained in the predictors) and Q^2 (predictive accuracy via cross-validation). Cluster differences were assessed using Fisher distance and corresponding p values. The model's predictive power was further validated on cross-validation and test datasets by calculating the percentage of correctly classified samples. Based on these statistical parameters and classification results, the most effective PLS-DA model was selected.

2.5.6 | The Principal Component Analysis

The full FTIR-ATR spectra were extracted based on their transmittance values to generate a comprehensive dataset for PCA. Several wavenumber ranges of 1000–650, 1500–1001, 2000–1501, 2500–2001, 3000–2501, 3500–3001 and 4000–3501 cm^{-1} were selected, as they represent both the functional group and fingerprint regions of the spectra. These spectral regions were chosen due to their high potential in capturing key molecular vibrations that can effectively distinguish between different sample groups, particularly for permissibility authentication purposes. Prior to PCA, the dataset was preprocessed using the Pareto scaling technique, which centres the data and scams each variable by the square root of its standard deviation. This method enhances moderate variations while preserving the data structure, making it particularly suitable for spectroscopic analysis. As a result of Pareto scaling, the distribution of the variables approached normality through the Gaussian distribution of the transformed data. The number of PCs was optimised to obtain optimum differentiation among samples. The differentiation result of samples was observed using PCA score plot. Moreover, PCA model was evaluated using its R^2 and Q^2 value to justify the good of fitness and predictivity of the PCA model, respectively [18].

2.5.7 | Limit of Detection (LOD) and Limit of Quantification (LOQ)

To establish the analytical sensitivity of the FTIR-ATR method, the LOD and LOQ were determined from the PLS regression calibration model built using the fingerprint region of 1000–650 cm^{-1} from the XLSTAT software. A univariate calibration curve was constructed by plotting the predicted lard concentration (%v/v) against the reference concentration values. The LOD and LOQ were calculated according to the ICH Q2(R1) guideline using the following equation:

$$LOD = \frac{3.3\sigma}{S} \tag{1}$$

and

$$LOQ = \frac{10\sigma}{S} \tag{2}$$

where σ is the residual standard deviation of the regression line and S is the slope of the calibration curve. Additionally, a multivariate LOD was estimated as 3 × RMSECV derived from the

PLS cross-validation results, consistent with established multivariate figures-of-merit approaches [19].

3 | Results and Discussion

3.1 | Colour Analysis of Thermally Treated Lard-Adulterated PO

Table 1 shows the ANOVA of the colour analysis of the oil sample, in which the adulteration by lard significantly influences the colour properties of the palm oil after thermal exposure. The addition of lard led to significant changes in the L^*, a^* and b^* values even at low concentrations ($\geq 10\%$), especially at frying temperatures above 150°C. These trends indicate that colour degradation is concentration dependent and increases under thermal stress. The L^* value, which represents lightness, generally decreased with increasing temperature, especially for oil blends containing 30%–50% lard [20]. This decrease is due to thermal degradation and polymerisation reactions during heating, resulting in a darker oil shade. For example, the 50% lard blend showed a decrease in L^* from 43.15 at 0°C to 35.73 at 200°C. These results are consistent with previous studies, such as Zhuang et al. [20], who reported decreasing L^* values in frying oils due to Maillard reaction and oxidation reactions at high temperatures. However, pure palm oil and blends with 1%–10% lard showed relatively stable L^* values at different temperatures, suggesting that small amounts of lard adulteration may not be visually detectable under mild thermal conditions.

The a^* value, which indicates the red-green hue, increased significantly in samples with a higher lard content and at higher temperatures. Palm oil blends with 30%, 40% and 50% lard showed a^* values above 0.9 at 200°C, whereas pure palm oil and less adulterated samples remained below 0.5. The b^* values (yellowing) were highest for pure lard and blends with moderate lard concentrations. These changes can be attributed to the altered fatty acid composition, the reduced antioxidant capacity and the accelerated oxidative degradation caused by the addition of lard [20]. These results suggest that colour analysis can be used as a preliminary method for permissibility authentication, as the unintentional or intentional presence of pork-derived ingredients such as lard in foods raises significant religious and ethical concerns among Muslim consumers. The result suggests that colorimetric analysis could serve as a rapid, initial screening tool to detect possible adulteration in processed oils. However, because ANOVA also shows that slight adulteration ($\leq 10\%$) does not cause statistically clear colour changes when slightly heated, colour analysis alone is not sufficient for reliable permissibility authentication. Thus, although ANOVA confirms its potential utility as a preliminary approach, robust verification must be achieved by integrating colour analysis with FTIR-ATR spectroscopy and chemometric methods for sensitive and accurate detection of narrow adulteration.

3.2 | FTIR-ATR Spectral Characterisation of Pure and Adulterated Oil Samples

The application of FTIR-ATR spectroscopy as a spectral biosensing technology enables rapid, nondestructive and label-free monitoring of molecular variations in edible oils. Coupling with chemometric analysis, the biosensing approach allows sensitive discrimination between pure and lard-adulterated PO, offering a practical platform for permissibility authentication under real processing conditions [21]. The FTIR-ATR spectra of PO, lard and oil adulterated mixture exhibited characteristic absorption bands associated with triglyceride structure and fatty acid composition [22]. In agreement with previous reports on edible fats and oils whereby the three prominent regions dominated the spectra of (i) the C–H stretching region (3000–2800 cm^{-1}), (ii) the carbonyl stretching region (1745–1740 cm^{-1}) and (iii) the fingerprint region (1500–650 cm^{-1}) [7], the C–H stretching bands at ~2900 cm^{-1} of asymmetric CH_2 stretching and ~2850 cm^{-1} of symmetric CH_2 stretching are attributed to methylene groups in the long aliphatic chains of triglycerides. The lard displayed slightly higher intensities in these bands compared to PO, consistent with its higher proportion of long-chain saturated fatty acids [23]. The C=O ester carbonyl stretching vibration appeared strongly near 1744 cm^{-1} in both oils, but its relative intensity and sharpness varied with adulteration level and thermal treatment. This variation reflects changes in the glyceride's ester environment due to the differing unsaturation levels between palm oil and lard.

The effect of heat treatment on the chemical composition of oil samples was represented in the FTIR spectra in Figures 1 and 2 using oil sample mixed with 20% lard at different temperature ranges. In the fingerprint region, PO and lard showed almost similar spectral patterns, particularly for CH_2 bending at ~1465 cm^{-1} and C-O-C stretching at ~1160 cm^{-1}. The latter is associated with ester linkages in triglycerides and is sensitive to both fatty acid composition and oxidation status [24]. A notable feature of the heat-treated samples was the weakening and broadening of the C-O-C and C=O bands, which is consistent with the hydrolysis and oxidation reactions reported for heated oils [25]. Notably, the peaks near ~1400 cm^{-1} correspond to a fluctuating CH_2 wagging or a symmetric -COO vibration, whereas a weak atmospheric CO_2 band was observed around 2400 cm^{-1}, consistent with previous FTIR-ATR literature [26]. These spectral assignments are consistent with established FTIR-ATR studies of lipid adulteration. The differences in peak positions and intensities between pure and adulterated samples, particularly in the carbonyl and fingerprint regions at 1745 and 1000–650 cm^{-1}, provided the chemical basis for the strong classification performance obtained with the DA and PLS-DA models. Previous work has also shown that the fingerprint region is best suited to discriminate between animal and vegetable fats, making it the most robust spectral window for permissibility authentication in thermally processed oils [27].

Importantly, these FTIR spectral changes are a direct expression of the mechanism of fatty acid oxidation, as the initiation, propagation and termination of the free radical reactions generate carbonyl and ester products that alter the vibrational signatures of the oils. To better illustrate this process, Figure 3 shows the autoxidation pathway of unsaturated fatty acids underlying the spectral shifts observed in pure and adulterated samples.

Oxidation of fatty acids, also known as autoxidation, is a chemical process that degrades the quality of oils and leads to rancidity

TABLE 1 | The ANOVA of colour analysis oil-adulterated lard blends at different temperature.

Oil sample	Temperature (°C)	*L**	*a**	*b**
100% lard	0	47.19 ± 1.80^{a}	0.03 ± 0.02^{a}	5.94 ± 0.43^{ab}
	50	43.24 ± 1.28^{a}	0.55 ± 0.04^{c}	5.53 ± 0.07^{ab}
	100	44.34 ± 0.10^{a}	0.35 ± 0.02^{bb}	5.38 ± 0.02^{a}
	150	45.27 ± 0.60^{a}	0.45 ± 0.02^{bc}	6.01 ± 0.14^{ab}
	200	44.79 ± 2.02^{a}	0.5 ± 0.06^{c}	6.06 ± 0.42^{b}
100% PO	0	40.21 ± 0.36^{a}	0.21 ± 0.12^{a}	2.76 ± 0.29^{a}
	50	43.97 ± 1.87^{bc}	0.36 ± 0.15^{a}	4.26 ± 0.49^{b}
	100	45.28 ± 0.93^{c}	0.27 ± 0.05^{a}	3.96 ± 0.09^{b}
	150	42.34 ± 0.83^{abc}	0.44 ± 0.11^{ab}	4.03 ± 0.15^{b}
	200	41.42 ± 0.57^{ab}	0.79 ± 0.12^{b}	4.20 ± 0.19^{b}
1% lard + 99% PO	0	43.71 ± 0.75^{ab}	0.04 ± 0.04^{a}	5.82 ± 0.09^{a}
	50	44.87 ± 1.13^{b}	0.16 ± 0.04^{a}	5.71 ± 0.25^{a}
	100	42.95 ± 0.51^{ab}	0.35 ± 0.07^{ab}	5.35 ± 0.01^{a}
	150	39.54 ± 1.96^{a}	0.75 ± 0.23^{bc}	5.02 ± 1.18^{a}
	200	40.12 ± 1.86^{ab}	0.94 ± 0.24^{c}	4.77 ± 1.22^{a}
5% lard + 95% PO	0	48.42 ± 1.72^{c}	0.09 ± 0.05^{a}	4.85 ± 1.31^{a}
	50	43.16 ± 0.41^{b}	0.30 ± 0.06^{a}	5.56 ± 0.07^{a}
	100	41.63 ± 0.20^{ab}	0.43 ± 0.02^{ab}	5.62 ± 0.00^{a}
	150	38.31 ± 1.60^{a}	0.90 ± 0.18^{c}	4.37 ± 1.17^{a}
	200	40.12 ± 0.57^{ab}	0.70 ± 0.09^{bc}	5.77 ± 0.34^{a}
10% lard + 90% PO	0	45.87 ± 1.04^{a}	0.06 ± 0.04^{a}	5.67 ± 0.28^{a}
	50	42.37 ± 0.20^{a}	0.48 ± 0.03^{b}	5.51 ± 0.04^{a}
	100	40.98 ± 0.43^{a}	0.68 ± 0.06^{b}	5.69 ± 0.14^{a}
	150	39.77 ± 1.51^{a}	0.72 ± 0.20^{b}	5.33 ± 0.67^{a}
	200	40.70 ± 0.89^{a}	0.74 ± 0.13^{b}	5.82 ± 0.21^{a}
20% lard + 80% PO	0	45.12 ± 1.96^{a}	0.26 ± 0.14^{a}	5.87 ± 0.01^{a}
	50	42.26 ± 1.04^{a}	0.58 ± 0.10^{ab}	5.81 ± 0.08^{a}
	100	41.19 ± 0.6^{a}	0.65 ± 0.02^{b}	5.85 ± 0.06^{a}
	150	41.81 ± 1.03^{a}	0.61 ± 0.10^{b}	5.98 ± 0.16^{a}
	200	44.21 ± 2.34^{a}	0.58 ± 0.04^{ab}	6.27 ± 0.10^{b}
30% lard + 70% PO	0	45.24 ± 0.85^{c}	0.28 ± 0.03^{a}	5.99 ± 0.08^{a}
	50	40.46 ± 1.72^{b}	0.70 ± 0.29^{ab}	5.26 ± 0.23^{b}
	100	40.14 ± 0.93^{b}	0.78 ± 0.05^{ab}	5.88 ± 0.38^{b}
	150	37.95 ± 1.52^{ab}	1.01 ± 0.14^{b}	4.64 ± 1.08^{b}
	200	35.54 ± 0.92^{a}	0.91 ± 0.13^{b}	0.92 ± 0.79^{b}
40% lard + 60% PO	0	43.91 ± 1.03^{a}	0.21 ± 0.00^{a}	4.23 ± 0.91^{a}
	50	41.28 ± 1.83^{a}	0.45 ± 0.37^{ab}	3.55 ± 0.14^{a}
	100	39.43 ± 1.33^{a}	0.99 ± 0.14^{b}	3.99 ± 0.45^{a}

(Continues)

TABLE 1 | (Continued)

Oil sample	Temperature (°C)	*L**	*a**	*b**
	150	41.20 ± 2.20^{a}	0.43 ± 0.26^{ab}	3.90 ± 0.27^{a}
	200	38.7 ± 1.00^{a}	1.15 ± 0.08^{b}	4.07 ± 0.29^{a}
50% lard + 50% PO	0	43.15 ± 0.15^{c}	0.36 ± 0.04^{a}	4.19 ± 0.33^{b}
	50	42.83 ± 1.57^{c}	0.38 ± 0.33^{ab}	3.70 ± 0.20^{ab}
	100	40.18 ± 0.70^{bc}	0.7 ± 0.07^{ab}	3.90 ± 0.27^{b}
	150	37.32 ± 0.74^{ab}	1.00 ± 0.18^{ab}	3.46 ± 1.06^{ab}
	200	35.73 ± 0.97^{a}	1.03 ± 0.15^{b}	2.16 ± 0.87^{a}

Note: The result presented in the mean value ± standard deviation ($n = 3$). Values in the same column with different superscript letters are significantly different at $p < 0.01$.

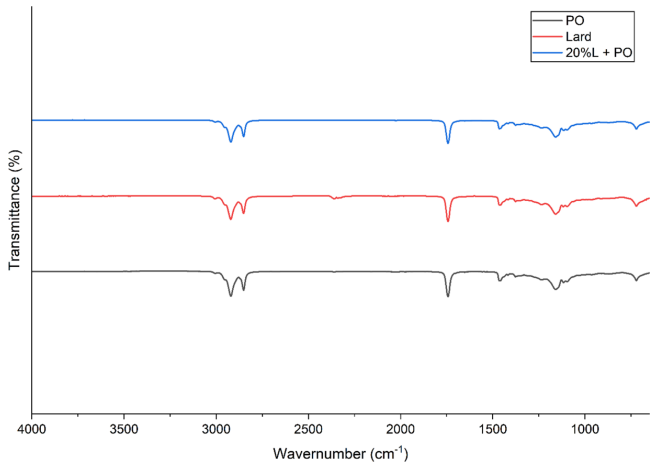

FIGURE 1 | The FTIR-ATR spectra of PO, lard and 20% lard + PO.

of the oil itself [29]. The process occurs as a chain reaction of free radicals that involves three main phases: initiation, propagation and termination. In the initial phase, an external factor, for example, heat, causes the unsaturated fatty acid (represented as FAH) to lose a hydrogen atom. In PO, this typically occurs with its unsaturated components such as oleic acid or linoleic acid. This loss leads to an extremely unstable and reactive fatty acid radical (FA•). In the subsequent propagation phase, known as the self-sustaining cycle, most of the damage occurs as the FA• reacts rapidly with atmospheric O_2 to form a fatty acid peroxyl radical (FA-OO•). This new, highly reactive peroxyl radical then attacks another stable FAH in the PO and removes a hydrogen atom from it. This reaction thus produces a fatty acid hydroperoxide (FA-OOH) and, above all, a new FA•. This new radical can now react with O_2, repeat the cycle and continue the chain reaction. The FA-OOH are unstable primary oxidation products as they decompose easily, especially by heat, and turn into secondary products such as aldehydes and ketones. These carbonyl groups are the cause of the undesirable 'bad' taste and rancid odour in degraded oil.

The chain reaction is finally stopped when the free radicals are neutralised or 'quenched'. This occurs when two radicals combine to form a stable, nonradical molecule. More importantly, the termination of the chain reaction is greatly aided by antioxidants (represented as AH). Because PO is naturally rich in powerful antioxidants such as tocopherols and tocotrienols (vitamin E), these molecules readily donate a hydrogen atom to the free radicals FA• and FA-OO•, neutralising them and stopping the propagation cycle. The antioxidant itself becomes a stable, less reactive radical (A•), which effectively interrupts the chain reaction and protects the oil from rapid degradation.

3.3 | Discriminant Analysis of FTIR-ATR Spectral Data

DA of the FTIR-ATR spectral data over seven segmented wavenumber ranges of 1000–650, 1500–1001, 2000–1501, 2500–2001, 3000–2501, 3500–3001 and 4000–3501 cm^{-1} yielded robust classification models for detecting adulteration in lipid-based samples, as shown in Table 2. The DA models showed exceptional performance, highlighted by high observation values and statistically significant Wilks' lambda test results ($p < 0.0001$) for all spectral ranges, indicating strong discriminatory power between adulterated and empty clusters. In particular, the 2500–2001 cm^{-1} region exhibited the highest $F_{observed}$ value of 504114.36, which significantly exceeded the $F_{critical}$ value of 577.48, characterising it as the most influential spectral window in terms of group separation. This region typically corresponds to combination bands and overtone vibrations associated with –CH-, $-CH_2$- and $-CH_3$- groups, which are abundant in lipid structures and often altered in adulterated formulations [30].

In all wavenumber segments, the training and cross-validation datasets achieved 100% classification accuracy for both adulterated and nonadulterated samples, with minimal exceptions. This demonstrates the excellent robustness and reproducibility of the model. In particular, the three wavenumber ranges 1000–650, 2000–1501 and 4000–3501 cm^{-1} provided a perfect classification of 100% during the training, validation and cross-validation phases, indicating that these ranges contain the most chemically significant features for the detection of adulteration. The 1000–650 cm^{-1} region is known as the 'fingerprint region' due to its compound-specific spectral complexity, making it highly diagnostic for compound identification and mixture discrimination. Similarly, the 4000–3501 cm^{-1} range, although less explored, includes N-H and O-H stretching vibrations that are likely to contain moisture, proteinaceous adulterants or other

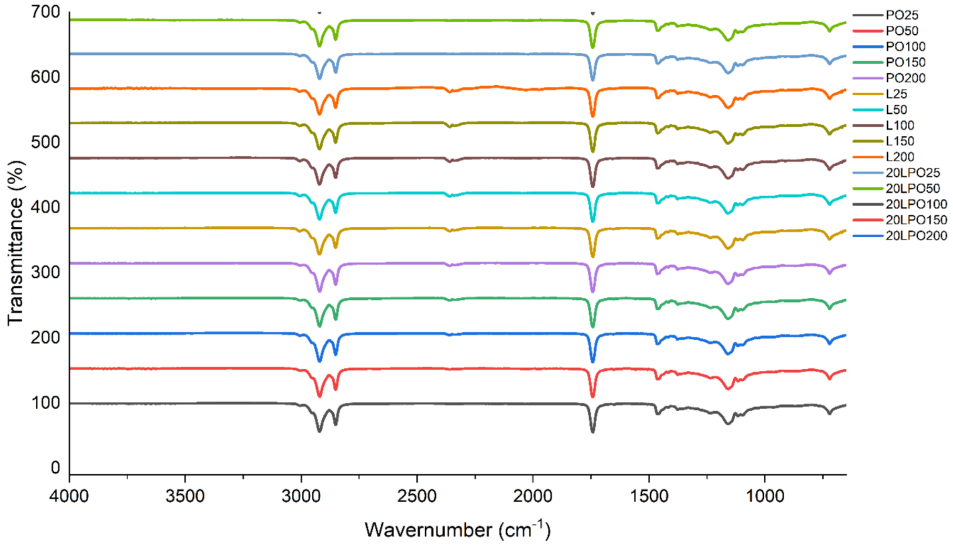

FIGURE 2 | The FTIR-ATR spectra of PO, lard and 20% lard + PO at different heating temperatures (25°C–200°C).

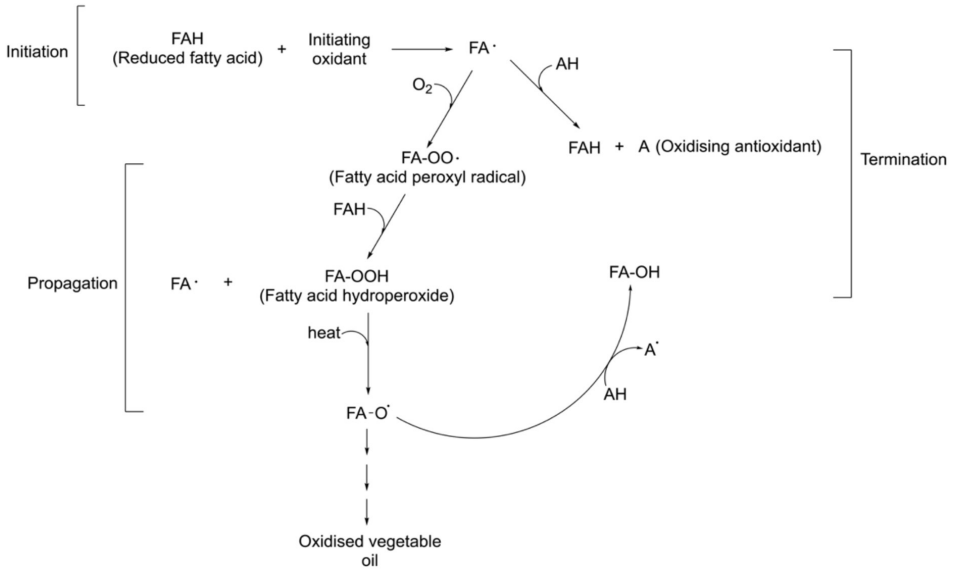

FIGURE 3 | The simplified mechanism of autoxidation of fatty acid cause through the external factor of heat [28].

polar constituents and provide additional distinguishing features [31].

Interestingly, the validation accuracy for the adulterated samples in the 1500–1001, 2000–1501, 2500–2001 and 3000–2501 cm^{-1} regions dropped to 0%. These misclassifications could indicate spectral interference or overfitting during training, suggesting that these regions contain discriminatory information but may require more refined preprocessing or model optimisation. For example, the 1500–1001 cm^{-1} region is rich in absorbances of the C=C and C=O functional groups present in both native and adulterated lipids, possibly leading to spectral overlap. Despite these anomalies, cross-validation performance in the same regions again reached an accuracy of 100%, indicating the overall generalisability of the model and the need for further calibration of the validation dataset. An important observation is the performance in the 3500–3001 cm^{-1} regions, where the cross-validation accuracy dropped slightly to 97.12% for adulterated samples and 96.67% for blank samples. Although this small deviation still indicates good performance, it may also indicate the presence of water-associated absorption or spectral noise in this higher energy range, which is more susceptible to external variables such as humidity or sample handling. This result is consistent with previous reports emphasising the need for a controlled environment when analysing high wavenumber spectra [32].

The apparent discrepancy between 0% validation accuracy and 100% cross-validation accuracy in several spectral regions of 1500–1001, 2000–1501, 2500–2001 and 3000–2501 cm^{-1} warrants clarification. In the XLSTAT's software DA framework, the 'validation' dataset refers to a small, fixed holdout subset automatically partitioned prior to model training, whereas 'cross-validation' employs a leave-one-out (LOO) procedure, iteratively removing each observation and rebuilding the model on the remaining samples. Given the high-dimensional nature of FTIR spectral data where the number of wavenumber variables substantially exceeds the number of observations,

TABLE 2 | Classification matrix of training, validation and cross-validation datasets of discriminant analysis of adulterated and blank samples of PO + lard at different FTIR-ATR wavenumber region of 4000–650 cm^{-1}.

Wavenumber discriminating model (cm^{-1})	Discriminating model quality Wilks' lambda test				Dataset	%Correct classification
	$F_{observed}$	$F_{critical}$	*p* value	Alpha		
1000–650	2247.71	3.56	< 0.0001	0.0001	Training	
					Adulterated	100
					Blank	100
					Validation	
					Adulterated	100
					Blank	0
					Cross-validation	
					Adulterated	100
					Blank	100
1500–1001	2330.46	3.68	< 0.0001	0.0001	Training	
					Adulterated	100
					Blank	100
					Validation	
					Adulterated	0
					Blank	100
					Cross-validation	
					Adulterated	100
					Blank	100
2000–1501	1077.74	3.17	< 0.0001	0.0001	Training	
					Adulterated	100
					Blank	100
					Validation	
					Adulterated	100
					Blank	0
					Cross-validation	
					Adulterated	100
					Blank	100
2500–2001	504,114.36	577.48	< 0.0001	0.0001	Training	
					Adulterated	100
					Blank	100
					Validation	
					Adulterated	0
					Blank	100
					Cross-validation	
					Adulterated	100
					Blank	100

(Continues)

TABLE 2 | (Continued)

Wavenumber discriminating model (cm^{-1})	Discriminating model quality Wilks' lambda test				Dataset	%Correct classification
	$F_{observed}$	$F_{critical}$	*p* value	Alpha		
3000–2501	169.57	2.54	< 0.0001	0.0001	Training	
					Adulterated	100
					Blank	100
					Validation	
					Adulterated	100
					Blank	0
					Cross-validation	
					Adulterated	97.12
					Blank	96.67
3500–3001	124.66	4.41	< 0.0001	0.0001	Training	
					Adulterated	99.04
					Blank	100
					Validation	
					Adulterated	100
					Blank	0
					Cross-validation	
					Adulterated	97.12
					Blank	96.67
4000–3501	2253.01	3.78	< 0.0001	0.0001	Training	
					Adulterated	100
					Blank	100
					Validation	
					Adulterated	100
					Blank	0
					Cross-validation	
					Adulterated	100
					Blank	100

the holdout validation subset can be insufficiently representative of the full sample distribution. Consequently, even one or two misclassified samples in a small holdout set produce 0% accuracy for a specific class. This is a recognised limitation of small external holdout sets in chemometric modelling. The LOO cross-validation, which uses all available training observations and is therefore more statistically robust for datasets of this size, consistently achieved 100% accuracy across the same regions, confirming the model's generalisation capacity. The 0% holdout validation accuracy in these regions therefore reflects the limitation of small partition size rather than a fundamental failure of the discriminant model. Notably, the fingerprint region (1000–650 cm^{-1}) achieved 100% accuracy across all three evaluation phases of training, validation and cross-validation, thus demonstrating its superiority as the most reliable spectral window for permissibility verification.

More importantly, these results highlight the utility of FTIR-ATR-DA models in food authentication, particularly in permissibility verification where nonpermissibility adulterants such as lard need to be reliably detected. The strong discrimination capability in both the fingerprint (1000–650 cm^{-1}) and overtone combination (2500–2001 cm^{-1}) ranges suggests that these bands should be prioritised for spectral monitoring and model optimisation. Furthermore, the consistency of the cross-validation results across all regions confirms the repeatability of the method and underlines the potential of FTIR-ATR spectroscopy as an analytical tool for permissibility compliance. The high

classification success also indicates the potential for real-time screening applications in the industry.

3.4 | Partial Least Squares–Discriminant Analysis of Adulterated Classification

This study also employed PLS-DA across seven distinct wavenumber regions ranging from 4000 to 650 cm^{-1}, with each region evaluated through multiple quality parameters that collectively provide insights into the model's discriminative capabilities as shown in Table 3, respectively. The analysis framework incorporated three critical evaluation metrics of R^2Y representing the model's fitness to dependent variables, R^2X indicating the model's fitness to independent variables and Q^2 quantifying the model predictive capability. Notably, all analysed regions demonstrated statistical significance with p values <0.01, establishing strict protocol for model reliability for permissibility verification across the FTIR-ATR spectral ranges [33]. Among the tested regions, the spectral window from 1000 to 650 cm^{-1} provided the most robust discriminant model, as evidenced by a high cumulative R^2Y of 0.895, R^2X of 1.000 and Q^2 of 0.893, all supported by a significant permutation test p value of 0.0001 as shown in Table 3. Notably, this model achieved 100% correct classification in both training and validation datasets, indicating the model could perfectly distinguish adulterated from blank samples in both known (training) and unseen (validation) datasets.

The superiority of this region is chemically justifiable as it encompasses the 'fingerprint region' whereby specific functional group vibrations particularly from ester carbonyls of C=O, C–O

TABLE 3 | Classification matrix of training and validation datasets of partial least squares-discriminant analysis of adulterated and blank samples of PO + lard at different FTIR-ATR wavenumber region of 4000–650 cm^{-1}.

Wavenumber discriminating model (cm^{-1})	Discriminating model quality R^2Y, R^2X and Q^2 cumulated indices and permutation test				Dataset	%Correct classification
	R^2Y	R^2X	Q^2	p value		
1000–650	0.895	1	0.893	<0.0001	Training	
					Adulterated	100
					Blank	100
					Validation	
					Adulterated	100
					Blank	0
1500–1001	0.009	0.911	0.009	<0.0001	Training	
					Adulterated	100
					Blank	0
					Validation	
					Adulterated	100
					Blank	0
2000–1501	0.368	0.268	0.224	<0.0001	Training	
					Adulterated	100
					Blank	100
					Validation	
					Adulterated	100
					Blank	0
2500–2001	0.489	0.358	0.474	<0.0001	Training	
					Adulterated	100
					Blank	100
					Validation	
					Adulterated	100
					Blank	53.33

(Continues)

TABLE 3 | (Continued)

Wavenumber discriminating model (cm^{-1})	Discriminating model quality R^2Y, R^2X and Q^2 cumulated indices and permutation test				Dataset	%Correct classification
	R^2Y	R^2X	Q^2	p value		
3000–2501	0.21	0.082	0.145	< 0.0001	Training	
					Adulterated	98.08
					Blank	13.33
					Validation	
					Adulterated	100
					Blank	0
3500–3001	0.332	0.997	0.279	< 0.0001	Training	
					Adulterated	100
					Blank	46.67
					Validation	
					Adulterated	100
					Blank	0
4000–3501	0.38	0.785	0.253	< 0.0001	Training	
					Adulterated	99.04
					Blank	50
					Validation	
					Adulterated	100
					Blank	0

stretching and aliphatic CH bending, which are known to vary between animal and plant fats [34]. These differences are crucial for permissibility authentication and verification, where the detection of porcine derivatives such as lard is of utmost importance. Other regions such as 2500–2001 and 3500–3001 cm^{-1} showed moderate model quality with R^2Y values of 0.489 and 0.332, respectively, and Q^2 values not exceeding 0.474. These areas of wavenumbers mainly capture overtone bands of O–H or N–H stretching, which may contribute to class separation but lack the specificity needed for precise classification. In contrast, the 1500–1001 and 3000–2501 cm^{-1} regions exhibited very poor model performance ($Q^2 = 0.009$ and 0.145) despite some models showing high R^2X values. This discrepancy suggests potential overfitting, where the model explains noise rather than meaningful variations, or that these spectral ranges are less informative due to overlapping bands and nonspecific absorptions. Such a discrepancy highlights the importance of validating PLS-DA models not only by internal metrics but also through external validation accuracy, especially in food authentication contexts where prediction of unknown samples is crucial [35].

The same overfitting concern also applies to FTIR-ATR region of 3000–2501 cm^{-1} where training classification accuracy for adulterated samples was 98.08% but, for blank samples, it dropped drastically to 13.33%. Although the Q^2 was slightly better at about 0.145, the disproportionate misclassification of blank samples signals low model reliability. Noteworthy, the % correct classification provides an intuitive and critical measure of model success in PLS-DA beyond the statistical fit indices. The ability of the model to correctly assign labels in both training and validation phases confirms its practical utility for real-world applications. In this study, the 1000–650 cm^{-1} range demonstrates the highest potential for permissibility verification and authentication through the FTIR-ATR by offering a balance of chemical specificity, statistical strength and reliable classification performance.

3.5 | The Principal Component Analysis and Sample Clustering

The PCA was applied as an unsupervised exploratory tool to visualise clustering patterns and identify natural variance in the FTIR-ATR data before the model training. The PCA score plot as shown in Figure 4 picture clear separation between adulterated and blank PO samples along the first two PCs (PC1 and PC2), which together accounted for a substantial proportion of total variance in the range of 91.19%–99.93%. PCA plays a pivotal role in chemometric workflows, as it allows for data dimensionality reduction while preserving essential variance and assists in identifying potential outliers or misclassification early in the analysis. Noteworthy, the KMO test of sampling adequacy for the FTIR-ATR spectra of 4000–650 cm^{-1} was found to be in the range of 0.950–0.956. According to the commonly accepted interpretation scale proposed, the KMO

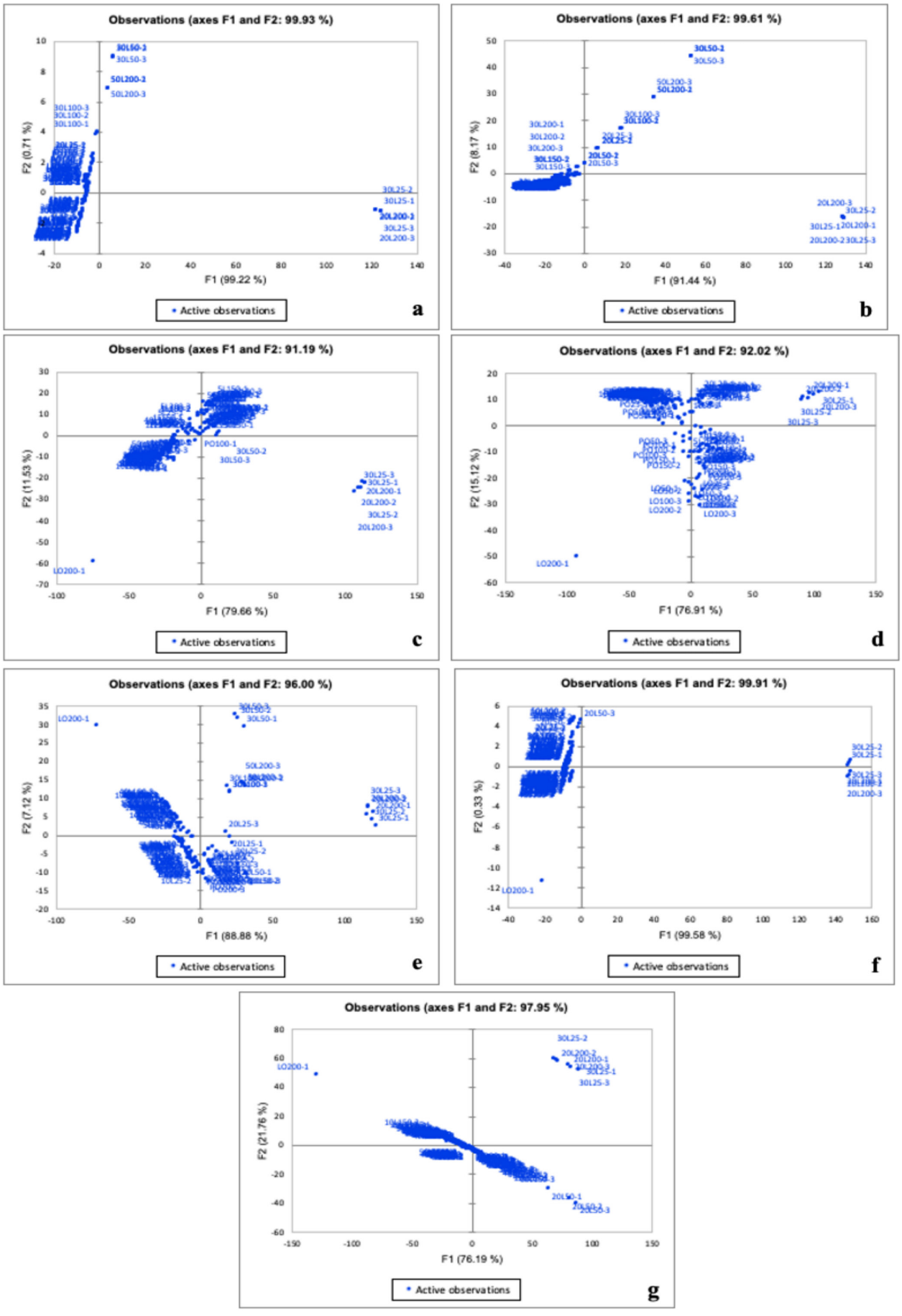

FIGURE 4 | Legend on next page.

FIGURE 4 | Combined PCA score plots of all FTIR-ATR dataset transformation of the wavenumber region of 4000–650 cm^{-1} of adulterated PO + lard and blank PO and lard. The FTIR-ATR wavenumber regions of (a) 650–1000 cm^{-1}; (b) 1500–1001 cm^{-1}; (c) 2000–1501 cm^{-1}; (d) 2500–2001 cm^{-1}; (e) 3000–2501 cm^{-1}; (f) 3500–3001 cm^{-1}; and (g) 4000–3501 cm^{-1}.

value above 0.9 categorised as excellent, indicating that the dataset is highly suitable for factor analysis and multivariate statistical evaluation. Such high values demonstrate that the intercorrelations among the FTIR-ATR variables are sufficiently compact, thus supporting the appropriateness of application such as PCA for pattern recognition and classification purposes [36]. Additionally, PCA helps to guide the selection of wavenumber regions for supervised modelling like PLS-DA by indicating which ranges carry the most discriminative studies. In this study, the PCA supported the supervised findings from PLS-DA confirming that adulterated and blank PO samples possess significantly different FTIR-ATR spectral patterns. The effective separation of classes without prior labelling underscores the suitability of FTIR-ATR coupled with PCA for preliminary screening in permissibility verification applications. Moreover, this separation suggests that the adulteration of lard introduces distinct spectral features in the FTIR-ATR fingerprint, which PCA can extract and represent in a low-dimensional space. The compact clustering of replicate samples within each group also highlights the reproducibility and consistency of spectral data across the samples.

Based on PCA in Figure 3, distinct clustering patterns were observed between adulterated PO samples and lard at different temperatures (25°C, 35°C and 200°C). Specifically, samples containing 20% and 30% lard adulteration in PO exhibited pronounced separation from pure PO clusters, particularly at elevated temperatures. This significant clustering can be attributed to the temperature-induced alterations in the molecular structure and functional groups of the fatty acids present in both lard and PO. The increase in temperature enhances the kinetic energy of lipid molecules, leading to the breakdown of triglycerides and the acceleration of lipid oxidation processes. The lipid oxidation primarily affects the aliphatic chain structure and introduces new functional groups such as aldehydes, ketones and hydroperoxides, which are readily detectable by FTIR-ATR spectroscopy. These oxidative changes result in spectral variations, especially in the regions associated with C=O stretching (1750–1745 cm^{-1}), $-CH_2-$ bending (1465 cm^{-1}) and C–O–C stretching vibrations (1160–1120 cm^{-1}) as reported beforehand [37]. The clustering of samples within the same group (adulterated or blank) was found to be tightly grouped, reflecting high reproducibility and low-group variation, which is desirable in spectral analysis. The adulterated samples exhibited distinct trajectories in the PCA plot, likely due to characteristic absorbance shifts caused by lard-specific functional groups such as saturated fatty acids, monoacylglycerols and diacylglycerols and carboxylic esters, which are chemically different from those in PO [38, 39]. From a chemometric standpoint, the successful discrimination seen in the PCA score plot confirms that the spectral variation introduced by adulteration is systematic rather than random, thus validating the potential of FTIR-ATR as a frontline technique for permissibility verification prior to supervised modelling. Specifically, lard is rich in saturated fatty acids and contains unique ester functional groups that exhibit characteristic absorption bands, especially in the fingerprint region of 1000–650 cm^{-1}, which influence the overall variance structure [40].

3.6 | Chemometric Model Correlation and Permissibility Verification Performance

The results show that chemometrics of DA, PLS-DA and PCA demonstrated a synergistic approach for the robust verification of permissibility compliance in PO adulterated with lard, subjected to thermal processing [41]. Each model contributed uniquely to the interpretation and classification of FTIR-ATR spectral data, particularly in identifying adulteration of PO with lard. The high accuracy and consistent separation patterns across models affirm the potential of FTIR-ATR-based chemometrics as a comprehensive tool for permissibility authentication. The DA showed exceptionally strong performance across all seven spectral regions, with 100% classification accuracy in most regions and statistically significant Wilks' lambda results ($p < 0.0001$), highlighting the strong discriminatory power between adulterated and blank PO samples. Complementary to DA, PLS-DA demonstrated a supervised regression-based classifier, providing deeper insights into FTIR spectral data relationships. The performance was evaluated through the values of R^2Y, R^2X and Q^2. On the other hand, PCA, an unsupervised technique, provided foundational support to the results from DA and PLS-DA by visually demonstrating distinct clustering between adulterated and blank PO samples.

Taken together, the correlation between PCA, DA and PLS-DA results confirmed that FTIR-ATR spectroscopy combined with well-structured chemometrics models offers a comprehensive and powerful approach for detecting lard in PO for permissibility verification purposes. The consistent identification of the fingerprint region of 1000–650 cm^{-1} as the most informative across DA, PLS-DA and PCA models suggested its prioritisation in future research for further model development for food authentication. In PCA, this region's distinct features contribute to the significant separation of adulterated and pure samples. In DA and PLS-DA, this region consistently yielded the most robust classification models with perfect accuracy. This correlation highlights the chemical significance of the fingerprint region, which is rich in compound-specific vibrations from fatty acids and esters that differentiate animal fats like lard from vegetable oils like PO. Integrating PCA, DA and PLS-DA can improve the classification accuracy and robustness of the models. For instance, data fusion strategies combining chromatographic and spectral data have shown improved performance in classifying edible oils [42]. The use of PCA for initial classification followed by PLS-DA for supervised analysis ensures precise identification and quantification of adulteration, making it a reliable method for permissibility verification. Furthermore, the combination of unsupervised chemometrics (PCA) and supervised chemometrics (DA and PLS-DA) provided both exploratory and confirmatory insights, allowing for better model calibration and enhanced the confidence in classification outcomes [43]. The

TABLE 4 | Analytical figures of merit of the FTIR-ATR/PLS regression model for lard adulteration detection in PO across thermal treatment conditions.

Thermal treatment temperature (°C)	Coefficient of determination (R^2)	RMSE (%*v*/*v*)	Intercept (S)	LOD (%*v*/*v*)	LOQ (%*v*/*v*)
25	0.871	108.736	10,926.51	0.03	0.1
50	0.605	190.243	94,826.86	0.01	0.02
100	0.816	129.852	20,726.28	0.02	0.06
150	0.954	64.598	25,760.23	0.01	0.03
200	0.020	299.671	870.48	1.14	3.44

use of chemometrics techniques affirms the feasibility of FTIR-ATR spectroscopy as a frontline tool in industrial permissibility compliance systems, with potential applications in real-time adulteration screening and quality control of food products. In summary, the correlation between DA, PLS-DA and PCA is significant in the context of permissibility verification of adulterated edible oils. These methods complement each other, with PCA providing initial classification and DA as well as PLS-DA offering detailed supervised analysis, ensuring accurate and reliable detection of nonpermissibility components in food products.

3.7 | Limit of Detection and Limit of Quantification Across Thermal Conditions

Table 4 presents the LOD and LOQ of the FTIR-ATR/PLS method across five thermal treatment conditions calculated from the univariate calibration curve using the ICH Q2(R1) approach. The best model performance was observed at 150°C ($R^2 = 0.954$) providing the lowest LOD and LOQ, indicating that moderate-to-high thermal treatment enhances the spectral contrast between pure and lard-adulterated palm oil. This improvement is attributable to heat-induced lipid oxidation generating secondary carbonyl compounds such as aldehydes, ketones and ester-degradation products that amplify the FTIR fingerprint region signal proportional to lard concentration [44]. However, at 25°C, the R^2 of 0.871 indicates acceptable but moderate predictive performance of the FTIR-ATR instrument. The relative higher LOD at ambient temperature compared to 150°C suggests that without thermal activation, the spectral differences between lard and PO in the 1000–650 cm^{-1} fingerprint region are less pronounced, resulting in greater regression scatter and reduced sensitivity. This is consistent with the understanding that the fingerprint region becomes more diagnostically powerful when heat-induced molecular rearrangements produced structurally distinct oxidation products unique to lard's fatty acid composition.

The most notable finding is the sharp deterioration in model performance at 200°C where the R^2 collapsed to 0.020 indicating near-complete loss of predictive power and corresponding to the highest LOD and LOQ across all conditions. This is explained by the extreme thermal degradation occurring above 180°C where extensive polymerisation, hydrolysis and free-radical chain termination reactions produce overlapping spectral profiles that homogenise the chemical distinction between pure and adulterated samples. This finding emphasises a practical limitation of the FTIR-ATR/PLS method although thermally resilient up to 150°C; the method's quantitative sensitivity degrades significantly at deep-frying temperatures of 200°C, a point that should be acknowledged in real-world deployment scenarios. Nonetheless, the method demonstrates robust and sensitive detection across the practical culinary range of 25°C–150°C, covering the majority of standard food preparation conditions relevant to permissibility verification.

4 | Conclusion

This study confirmed that thermal processing significantly influences the colour and FTIR-ATR spectral characteristics of PO adulterated with lard. Despite the spectral complexity introduced by heating, chemometric approaches including PCA, DA and PLS-DA successfully discriminated between pure and adulterated samples (PO + lard) with high accuracy. The fingerprint region of 1000–650 cm^{-1} consistently emerged as the most reliable spectral window for permissibility verification, demonstrating strong discriminatory power across all models. The integration of FTIR-ATR spectroscopy with chemometric tools thus provides a robust, rapid and nondestructive method for detecting lard adulteration in PO under various thermal conditions. The developed FTIR-ATR and chemometric approach is therefore suitable for routine screening, as it reliably detects lard adulteration in thermally processed PO down to 1% *v*/*v* with LOD and LOQ ranges of 0.01%–1.14% and 0.02%–3.34% *v*/*v*. These findings highlight the potential of spectroscopic-chemometric strategies as practical solutions for strengthening permissibility authentication systems in the food industry.

Author Contributions

Muhammad Zulhelmi Nazri: conceptualisation, methodology, resources, formal analysis, investigation, writing – original draft, funding acquisition. **Dayang Norulfairuz Abang Zaidel:** validation, writing – review and editing, supervision, funding acquisition. **Muhamad Shirwan Abdullah Sani:** validation, writing – review and editing. **Hajar Aminah A. Karim:** methodology, formal analysis, investigation, writing – original draft. **Siti Nor Azlina Abd Rashid:** methodology, formal analysis, investigation, validation, writing – original draft. **Anjar Windarsih:** formal analysis, writing – original draft.

Acknowledgements

This research was funded by the Universiti Teknologi Malaysia (UTM) through the *Geran Penggalakan Inovasi Staf Pengurusan, Profesional dan Pelaksana* (I3P) (Grant No. R.J130000.7709.4J717) and the *Geran*

Penyelidikan Hi-Tech(F4) (Grant No. Q.K130000.4643.00Q41). The authors thanked the Innovation Centre in Agritechnology for Advanced Bioprocessing (ICA), UTM Pagoh Campus, for providing the facilities and supporting the permissibility research authentication and verification.

Funding

This work was supported by the Research Management Centre, Universiti Teknologi Malaysia (R.J130000.7709.4J717 and Q.K130000.4643.00Q41).

Conflicts of Interest

The authors declare no conflicts of interest.

Data Availability Statement

The data that support the findings of this study are available from the corresponding author upon reasonable request.

Peer Review

For transparency, the peer review documents associated with this article are available at https://doi.org/10.1002/cem.70137.

References

1. S. A. S. Z. Abidin, M. Nizar, N. N. A. Nizar, M. S. A. Shukor, R. Zainal, and S. R. A. Mutalib, "*Halal* Concerns on Lard in Food Products and Its Detection Methods," *Halalsphere* 3, no. 2 (2023): 79–90, https://doi.org/10.31436/hs.v3i2.72.

2. A. Choudhary, N. Gupta, F. Hameed, and S. Choton, "An Overview of Food Adulteration: Concept, Sources, Impact, Challenges and Detection," *International Journal of Chemical Studies* 8, no. 1 (2020): 2564–2573, https://doi.org/10.22271/chemi.2020.v8.i1am.8655.

3. M. N. Hussain, K. N. Basri, S. Arshad, S. Mustafa, M. F. A. Khir, and J. Bakar, "Analysis of Lard in Palm Oil Using Long-Wave Near-Infrared (LW-NIR) Spectroscopy and Gas Chromatography-Mass Spectroscopy (GC–MS)," *Food Analytical Methods* 16, no. 2 (2023): 349–355, https://doi.org/10.1007/s12161-022-02423-y.

4. R. M. H. R. Nhari, J. H. Soh, N. F. K. Mokhtar, N. A. Mohammad, and A. M. Hashim, "*Halal* Authentication Using Lateral Flow Devices for Detection of Pork Adulteration in Meat Products: A Review," *Food Additives & Contaminants: Part a* 40, no. 8 (2023): 971–980, https://doi.org/10.1080/19440049.2023.2242955.

5. M. A. Mousa, Y. Wang, S. A. Antora, et al., "An Overview of Recent Advances and Applications of FT-IR Spectroscopy for Quality, Authenticity, and Adulteration Detection in Edible Oils," *Critical Reviews in Food Science and Nutrition* 62, no. 29 (2022): 8009–8027, https://doi.org/10.1080/10408398.2021.1922872.

6. Q. Li, J. Chen, Z. Huyan, et al., "Application of Fourier Transform Infrared Spectroscopy for the Quality and Safety Analysis of Fats and Oils: A Review," *Critical Reviews in Food Science and Nutrition* 59, no. 22 (2019): 3597–3611, https://doi.org/10.1080/10408398.2018.1500441.

7. R. Jamwal, S. Kumari, S. Sharma, S. Kelly, A. Cannavan, and D. K. Singh, "Recent Trends in the Use of FTIR Spectroscopy Integrated With Chemometrics for the Detection of Edible Oil Adulteration," *Vibrational Spectroscopy* 113 (2021): 103222, https://doi.org/10.1016/j.vibspec.2021.103222.

8. A. Rohman and A. Windarsih, "The Application of Molecular Spectroscopy in Combination With Chemometrics for *Halal* Authentication Analysis: A Review," *International Journal of Molecular Sciences* 21, no. 14 (2020): 5155, https://doi.org/10.3390/ijms21145155.

9. F. Mabood, L. Ali, R. Boque, et al., "Robust Fourier Transformed Infrared Spectroscopy Coupled With Multivariate Methods for Detection and Quantification of Urea Adulteration in Fresh Milk Samples," *Food Science & Nutrition* 8, no. 10 (2020): 5249–5258, https://doi.org/10.1002/fsn3.987.

10. A. Hassoun, M. Carpena, M. A. Prieto, et al., "Use of Spectroscopic Techniques to Monitor Changes in Food Quality During Application of Natural Preservatives: A Review," *Antioxidants* 9, no. 9 (2020): 882, https://doi.org/10.3390/antiox9090882.

11. M. Z. Nazri, S. N. A. A. Rashid, S. A. Malik, H. A. A. Karim, M. S. A. Sani, and D. N. A. Zaidel, "The FTIR-ATR Spectroscopy and Multivariate Data Analysis (MVDA) for *Halal* Authentication of Animal Fatty Acids," *Malaysian Journal of Chemistry* 26, no. 6 (2024): 184–193, https://doi.org/10.55373/mjchem.v26i6.184.

12. I. Irnawati, A. Windarsih, A. W. Indrianingsih, et al., "Rapid Detection of Tuna Fish Oil Adulteration Using FTIR-ATR Spectroscopy and Chemometrics for *Halal* Authentication," *Journal of Applied Pharmaceutical Science* 13, no. 4 (2023): 231–239, https://doi.org/10.7324/JAPS.2023.120270.

13. A. Windarsih, N. K. A. Bakar, Dachriyanus, N. D. Yuliana, F. D. O. Riswanto, and A. Rohman, "Analysis of Pork in Beef Sausages Using LC-Orbitrap HRMS Untargeted Metabolomics Combined With Chemometrics for *Halal* Authentication Study," *Molecules* 28, no. 16 (2023): 5964, https://doi.org/10.3390/molecules28165964.

14. A. Rohman and Y. B. C. Man, "Analysis of Pig Derivatives for *Halal* Authentication Studies," *Food Reviews International* 28, no. 1 (2012): 97–112, https://doi.org/10.1080/87559129.2011.595862.

15. J. J. Zhang, X. Xu, Q. Zeng, et al., "Lipidomics and Metabolomics Reveal the Molecular Mechanisms Underlying the Effect of Thermal Treatment on Composition and Oxidative Stability of Walnut Oil," *Food Research International* 191 (2024): 114695, https://doi.org/10.1016/j.foodres.2024.114695.

16. P. Charuwat, G. Boardman, C. Bott, and J. T. Novak, "Thermal Degradation of Long Chain Fatty Acids," *Water Environment Research* 90, no. 3 (2018): 278–287, https://doi.org/10.2175/106143017X15131012152825.

17. Addinsoft. *XLSTAT Statistical and Data Analysis Solution (Version 2019)* (Addinsoft, 2025), https://www.xlstat.com.

18. M. Z. Nazri, N. A. Latiff, S. N. A. A. Rashid, et al., "Enzymatic and Microbial-Assisted Treatments for the Extraction of Agarwood Essential Oils and Authentication Using FTIR-ATR Spectroscopy and Multivariate Data Analysis," *Malaysian Journal of Chemistry* 27, no. 2 (2025): 197–216, https://doi.org/10.55373/mjchem.v27i2.197.

19. P. Borman and D. Elder, "Q2 (R1) Validation of Analytical Procedures: Text and Methodology," in *ICH Quality Guidelines: An Implementation Guide* (Wiley, 2017), 127–166, https://doi.org/10.1002/9781118971147.ch5.

20. Y. Zhuang, J. Dong, X. He, et al., "Impact of Heating Temperature and Fatty Acid Type on the Formation of Lipid Oxidation Products During Thermal Processing," *Frontiers in Nutrition* 9 (2022): 913297, https://doi.org/10.3389/fnut.2022.913297.

21. F. Munir, S. G. Musharraf, S. T. H. Sherazi, M. I. Malik, and M. I. Bhanger, "Detection of Lard Contamination in Five Different Edible Oils by FT-IR Spectroscopy Using a Partial Least Squares Calibration Model," *Turkish Journal of Chemistry* 43, no. 4 (2019): 1098–1108, https://doi.org/10.3906/kim-1902-17.

22. M. Z. Nazri, S. N. A. A. Rashid, N. A. Latiff, et al., "*Halal* Verification of Imported Fish Pellets by FTIR-ATR Spectroscopy Approach and Multivariate Data Analysis," *Journal of Advanced Research Design* 139, no. 1 (2026): 158–174, https://doi.org/10.37934/ard.139.1.158174.

23. X. Jiang, S. Li, G. Xiang, et al., "Determination of the Acid Values of Edible Oils via FTIR Spectroscopy Based on the OH Stretching Band,"

Food Chemistry 212 (2016): 585–589, https://doi.org/10.1016/j.foodchem.2016.06.035.

24. A. M. Salih, M. B. Ahmad, N. A. Ibrahim, et al., "Synthesis of Radiation Curable Palm Oil–Based Epoxy Acrylate: NMR and FTIR Spectroscopic Investigations," *Molecules* 20, no. 8 (2015): 14191–14211, https://doi.org/10.3390/molecules200814191.

25. M. Wang, J. Chen, B. Jing, L. Zhang, Y. Dong, and X. Yu, "Analysis of Reaction Kinetics of Edible Oil Oxidation at Ambient Temperature by FTIR Spectroscopy," *European Journal of Lipid Science and Technology* 122, no. 6 (2020): 1900302, https://doi.org/10.1002/ejlt.201900302.

26. R. Kumar, S. Lang, P. Englezos, and J. Ripmeester, "Application of the ATR-IR Spectroscopic Technique to the Characterization of Hydrates Formed by CO_2, CO_2/H_2 and $CO_2/H_2/C_3H_8$," *Journal of Physical Chemistry A* 113, no. 22 (2009): 6308–6313, https://doi.org/10.1021/jp901670e.

27. I. Barra, M. A. Mansouri, Y. Cherrah, M. Kharbach, and A. Bouklouze, "FTIR Fingerprints Associated to a PLS-DA Model for Rapid Detection of Smuggled Non-Compliant Diesel Marketed in Morocco," *Vibrational Spectroscopy* 101 (2019): 40–45, https://doi.org/10.1016/j.vibspec.2019.02.001.

28. T. E. V. Hoff, R. E. Harmon, Y. Orlova, J. J. Hermans, A. Gambardella, and P. D. Iedema, "Experimental Validation of a Reaction Network Model for Autoxidation of Linoleate Esters," *Progress in Organic Coatings* 189 (2024): 108363, https://doi.org/10.1016/j.porgcoat.2024.108363.

29. Y. Yang, D. Liu, W. Xing, C. Tang, X. Feng, and J. Zhang, "Simulating Fatty Acid Autoxidation and Exploring the Related Volatiles Formation Mechanism," *LWT* 214 (2024): 117083, https://doi.org/10.1016/j.lwt.2024.117083.

30. N. A. Porter, "A Perspective on Free Radical Autoxidation: The Physical Organic Chemistry of Polyunsaturated Fatty Acid and Sterol Peroxidation," *Journal of Organic Chemistry* 78, no. 8 (2013): 3511–3524, https://doi.org/10.1021/jo4001433.

31. M. Z. Nazri, S. N. A. A. Rashid, and D. N. A. Zaidel, "Fourier Transform Infrared (FTIR) Spectroscopy, Gas Chromatography and Chemometric Analysis for *Halal* Authentication in Food Products," *Journal of Academia* 13, no. 2 (2025): 209–233, https://doi.org/10.24191/joa.v13i1.

32. L. H. Nurani, F. D. O. Riswanto, A. Windarsih, C. A. Edityaningrum, A. Guntarti, and A. Rohman, "Use of Chromatographic-Based Techniques and Chemometrics for Halal Authentication of Food Products: A Review," *International Journal of Food Properties* 25, no. 1 (2022): 1399–1416, https://doi.org/10.1080/10942912.2022.2082468.

33. V. Maritha, P. W. Harlina, I. Musfiroh, A. M. Gazzali, and M. Muchtaridi, "The Application of Chemometrics in Metabolomic and Lipidomic Analysis Data Presentation for *Halal* Authentication of Meat Products," *Molecules* 27, no. 21 (2022): 7571, https://doi.org/10.3390/molecules27217571.

34. M. Lucarini, A. Durazzo, J. S. D. Pulgar, P. Gabrielli, and G. Lombardi-Boccia, "Determination of Fatty Acid Content in Meat and Meat Products: The FTIR-ATR Approach," *Food Chemistry* 267 (2018): 223–230, https://doi.org/10.1016/j.foodchem.2017.11.042.

35. A. Dashti, J. Müller-Maatsch, Y. Weesepoel, et al., "The Feasibility of Two Handheld Spectrometers for Meat Speciation Combined With Chemometric Methods and Its Application for *Halal* Certification," *Food* 11, no. 1 (2021): 71, https://doi.org/10.3390/foods11010071.

36. L. Chen, R. Chen, E. M. Atwa, et al., "Nutritional Quality Assessment of Miscellaneous Cassava Tubers Using Principal Component Analysis and Cluster Analysis," *Food* 13, no. 12 (2024): 1861, https://doi.org/10.3390/foods13121861.

37. M. Azir, S. Abbasiliasi, T. A. T. Ibrahim, Y. N. A. Manaf, A. Q. Sazili, and S. Mustafa, "Detection of Lard in Cocoa Butter—Its Fatty Acid Composition, Triacylglycerol Profiles, and Thermal Characteristics," *Food* 6, no. 11 (2017): 98, https://doi.org/10.3390/foods6110098.

38. N. A. S. Sapian, M. A. M. Roslan, A. M. Hashim, et al., "Differentiation of Lard From Other Animal Fats Based on *n*-Alkane Profiles Using Chemometric Analysis," *Food Research International* 164 (2023): 112332, https://doi.org/10.1016/j.foodres.2022.112332.

39. N. I. Azizan, N. F. K. Mokhtar, S. Arshad, et al., "Detection of Lard Adulteration in Wheat Biscuits Using Chemometrics-Assisted GCMS and Random Forest," *Food Analytical Methods* 14, no. 11 (2021): 2276–2287, https://doi.org/10.1007/s12161-021-02046-9.

40. H. Wasoh, N. A. S. Sapian, A. M. M. Fatin, et al., "Clustering Analysis and Differentiation of Lard From Palm Oil and Soybean Oil Based on *n*-Alkane and Triacylglycerides Profiles Using Chemometric Analysis," *Journal of Environmental Microbiology and Toxicology* 12, no. 2 (2024): 13–18, https://doi.org/10.54987/jemat.v12i2.1004.

41. M. Vergara-Barberán, M. J. Lerma-García, J. M. Herrero-Martínez, and E. F. Simó-Alfonso, "Cultivar Discrimination of Spanish Olives by Using Direct FTIR Data Combined With Linear Discriminant Analysis," *European Journal of Lipid Science and Technology* 117, no. 9 (2015): 1473–1479, https://doi.org/10.1002/ejlt.201400425.

42. E. Sufriadi, R. Idroes, H. Meilina, A. A. Munawar, Lelifajri, and G. Indrayanto, "Partial Least Squares-Discriminant Analysis Classification for Patchouli Oil Adulteration Detection by Fourier Transform Infrared Spectroscopy in Combination With Chemometrics," *ACS Omega* 8, no. 13 (2023): 12348–12361, https://doi.org/10.1021/acsomega.3c00080.

43. V. E. de Almeida, D. D. D. S. Fernandes, P. H. G. D. Diniz, et al., "Scores Selection via Fisher's Discriminant Power in PCA-LDA to Improve the Classification of Food Data," *Food Chemistry* 363 (2021): 130296, https://doi.org/10.1016/j.foodchem.2021.130296.

44. R. Zamora and F. J. Hidalgo, "Carbonyl-Phenol Adducts: An Alternative Sink for Reactive and Potentially Toxic Lipid Oxidation Products," *Journal of Agricultural and Food Chemistry* 66, no. 6 (2018): 1320–1324, https://doi.org/10.1021/acs.jafc.7b05360.